

ADVANCED PHOTOVOLTAIC MEASUREMENT TECHNIQUES

Lawrence L. Kazmerski
Solar Energy Research Institute
Golden, Colorado 80401, U.S.A.

A survey of measurement techniques for photovoltaic research is presented. Characterization methods are discussed covering three major areas: (1) Cell Performance; (2) Electro-Optical Measurements; and, (3) Materials Characterization. Examples are given from current solar cell research and development in amorphous, polycrystalline and single-crystal photovoltaic technologies.

Solar Cells, Photovoltaic Measurements

1. Introduction

The accurate determination of the controlling fundamental parameters and the operational characteristics is essential for the advancement of photovoltaic materials and device technologies. The needs for these measurements span the range from the analysis of the basic compositional and chemical properties of solar cell candidate materials to the evaluation of the operational performance of the completed devices¹⁻³. The end uses of such characterizations are primarily twofold: (i) to improve, understand or document the cell output characteristics (e.g., efficiency, open-circuit voltage, short-circuit current, etc.); and/or, (ii) to provide diagnostic information on the reliability, stability or failure mechanisms encountered in these cell technologies. In most cases, it is necessary to apply more than one measurement technique for the unambiguous solution of a problem³⁻⁵. The wide-range, cost and sophistication of the measurements required make it impossible for every solar

cell research group to be characterization-independent. Additionally, the "second party" verification procedure provides credibility and objectivity for reported results. These two factors have fostered the cooperative interaction among research groups and the establishment of multifunctional facilities to support research and development operations. This paper reviews the range of measurement technologies required for support of photovoltaic materials/device R&D. The emphasis is placed on measurement support needed to provide intermediate efficiency (i.e., $> 10\%$) thin-film (amorphous and polycrystalline) and high-efficiency (i.e., $> 20\%$) single-crystal and multiple junction solar cells. The purpose of this paper is not to provide an exhaustive description of each technique nor a detailed catalogue of all methods. However, a range of major measurements, their strengths and limitations, and the complementary application of these to cell problems are emphasized. Three major areas are covered: (1) Cell Performance; (2) Electro-Optical Measurements; and, (3) Materials Characterization. Throughout these discussions, the reader should realize the importance of the expertise required in the interpretation of results, and the required interaction and communication between the measurement and device/materials scientists.

2. Cell Performance

The final benchmark for a solar cell is its operational characteristics. The most-cited parameter for a device is its efficiency, the measure of its ability to convert the sun's radiation (photons) into useful electricity⁶. The ideal method for determining the performance of a cell might be thought to be an outdoor measurement--using the sun as the light source. However, changes in air mass conditions, atmospheric absorption and scattering, altitude and environmental particulates all affect the terrestrial solar irradiance⁷. Thus, the spectral distribution of "outdoor" sunlight varies widely with both location and time of day and year--making a measurement of a quantity such as cell efficiency both inaccurate and non-standard. In order to

AMO, ASTM-B5 Direct and Global Spectra

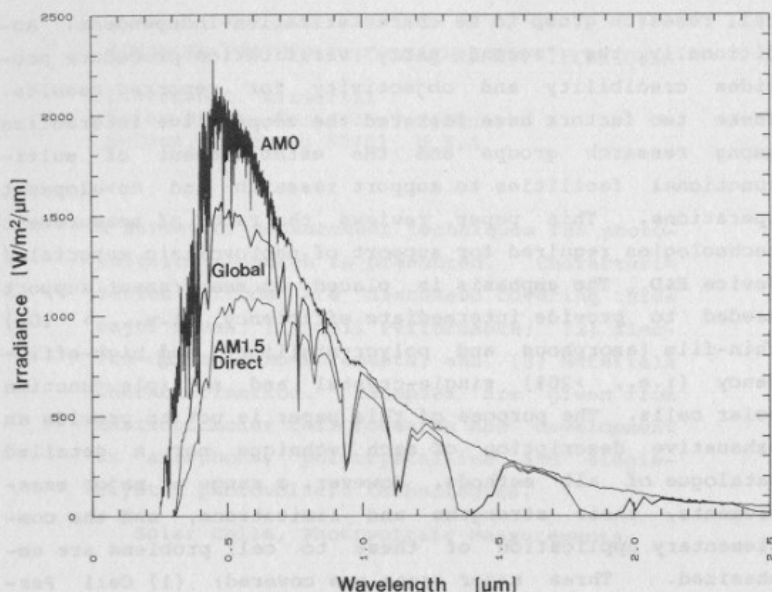


Fig. 1. Standard spectra for (a) AMO; (b) AM1.5 direct; and, (c) AM1.5 global.

Table 1. The effect of the spectral mismatch index method on reducing the error in indoor and outdoor measurements of the short circuit current. (From ref. 13 and 14.)

Cell	M	Outdoors		M	Simulator	
		%Error Uncorr.	%Error Corr.		%Error Uncorr.	%Error Corr.
Si	0.9979	-0.2	0.0	0.9985	-0.6	-0.5
CdS/CdTe	1.0174	1.6	-0.1	0.9767	-3.4	-1.1
GaAs	1.0006	0.0	-0.1	0.9881	-1.2	-0.9
CdS/CuInSe	0.9420	-5.3	0.6	0.9904	-2.6	-1.7
Si(amorp.)	1.0795	7.8	-0.2	1.1562	15.8	0.2

reproducibly measure the performance of a cell outdoors, these irradiance effects must be precisely determined. Although specific conditions can be set with respect to atmospheric conditions and irradiance levels, natural sunlight is not readily available as a standard reference. Using specified conditions, cell efficiencies can be determined outdoors--but the complex procedure involves approximately three days of measurement, and many hours of data reduction^{7,8}. It is the method used to establish calibrated, terrestrial standard solar cells, and is time-wise prohibitive for the routine evaluation of cell efficiency.

It should be emphasized that the determination of the solar cell efficiency depends critically on the spectral content of the source. The major effect is on the current produced. Three representative standard spectra are presented in Fig. 1. The AM0 (air-mass zero or outer space) spectrum is the one utilized for measurement of space cell technologies. For terrestrial applications, two choices are possible, both of which are designated as AM1.5 standards. The first is a direct spectrum, and has been considered as the standard since the mid-1970's since its establishment by NASA⁹. This spectrum contains no diffuse or scattered light components. It can be produced by placing a columnating tube over the cell during an outdoor measurement, and best typifies the light a concentrator cell would see during operation. It has always been recognized that the terrestrial spectrum has a significant scattered light component that affects the operational characteristics of a photovoltaics cell. However, since the atmospheric conditions accompanying such a spectrum having both a direct and a diffuse component depends so much on location and time, no standard spectrum has been implemented--until recently. Since flat-plate solar cell are designed to operated under a global spectrum¹⁰, the efficiency determination of such devices is now becoming common and several standards committees have adopted a standard global spectrum--shown in Fig. 1 and compared to the direct and AM0 spectra. A major difference in the global spectrum is the amount of blue (shorter wave-

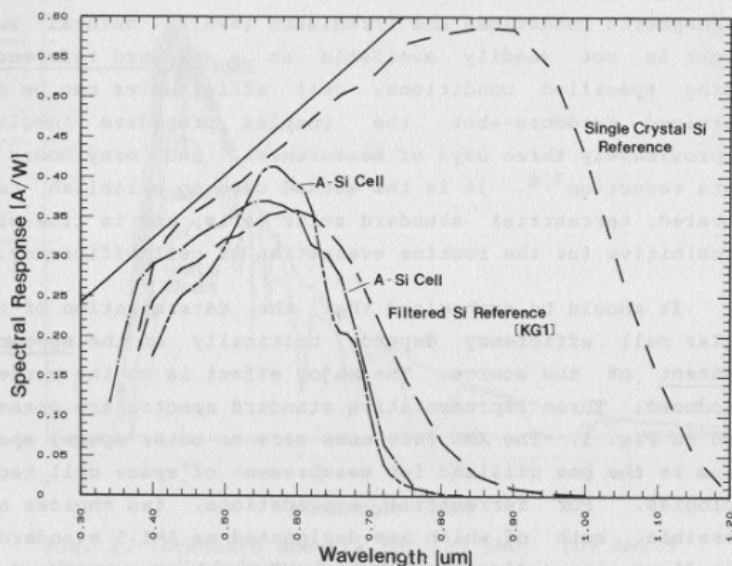


Fig. 2. Comparison of the spectral responses of several solar cells, including single crystal Si, amorphous Si, and a filtered single-crystal Si cell to simulate an amorphous Si standard.

length) response, especially important for some of the amorphous Si:H cell and higher bandgap III-IV alloy cell technologies. Among the major cell measurement laboratories, it is now accepted to provide a global spectrum efficiency for cells designed for a non-concentrator operation. Two points of interest are that a Si homojunction cell has the same efficiency under both direct and global spectra (set to the same power density), and lower bandgap cells lose some in efficiency due to a lowering in the red content of the global spectrum.

For reproducible and controlled determination of solar cell operating parameters, an artificial light source of a solar simulator is used. For such characterization, two methods can be employed. The first uses a reference solar cell and a light source closely matched to the solar spectrum (especially in the wavelength response range of the cell be analyzed)^{9,11}. The second method is more involved from the knowledge and measurement of the source's spectral content and the spectral response of the cell, but provides very accurate determinations of solar cell efficiency independent of the reference cell or light source^{12,13}.

The reference cell/light source method is the most common technique used by cell researchers. A reference cell, calibrated outdoors (either direct or global) is used to set the source irradiance, and the cell of interest is measured against this "standard". The calibration of the reference cell was originally established by NASA Lewis-Research Center⁹, and a new ASTM standard is currently being considered¹¹. Inherent to any such procedure is the assumption that the reference cell and the cell-under-test have essentially the same spectral response. Thus, for accuracy, reference cells of the same type must be employed in establishing similar irradiance levels. Until recently, only Si reference cells have been available. Using a Si reference cell with a 1.1 eV bandgap to measure a GaAsP cell with a 1.7 eV bandgap, leads to an error in the short-circuit current of 12-15%. Indications of this problem are provided in the comparisons of the spectral responses of several

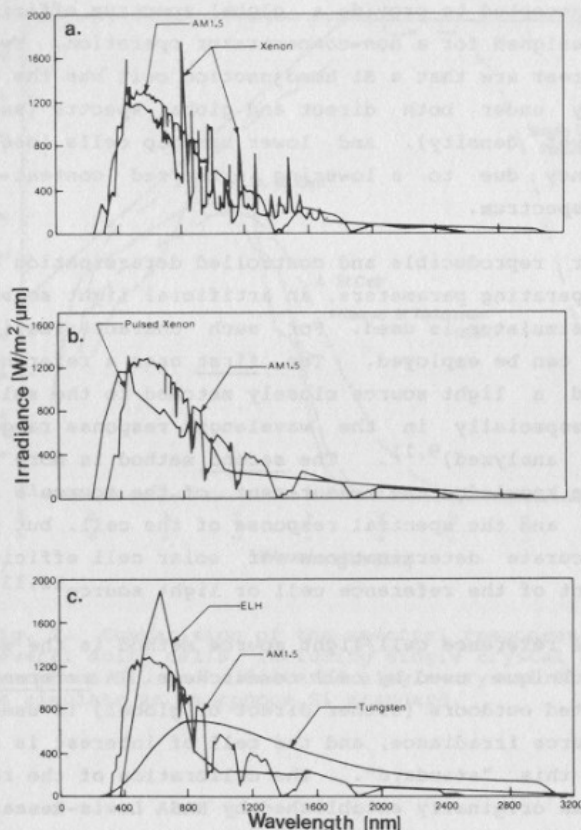


Fig. 3. Spectral distribution of various solar simulators shown with terrestrial sunlight spectrum (AM1.5): (a) short arc xenon lamp; (b) pulsed long arc xenon lamp; and, (c) ELH and tungsten lamps.

cells shown in Fig. 2. This source of error is now being minimized by using reference cells with similar spectral response. It is also assumed that the spectral contents of the simulator and the outdoor irradiance under standard conditions are the same. Figure 3 compares the spectra of several common simulator sources with the standard AM1.5 direct spectrum, and the differences are apparent. Careful, but expensive, filtering of sources can provide spectra close to the standard ones, but the use of light- and reference cell-independent techniques might be a simpler approach.

Two procedures can be used to reduce the error in the current determination that can accompany the calibrated reference cell method. The first procedure involves correcting the measured current for spectral mismatch errors¹², and is less sensitive to errors in spectral irradiance measurements. If the relative spectral response of the reference cell, $SR_R(\lambda)$, and the test cell $SR_T(\lambda)$, and the relative spectral irradiance of the source spectrum, $E_S(\lambda)$, can be measured, then the spectral mismatch error, M , can be computed from

$$M = \frac{\int SR_R(\lambda) E_{STND}(\lambda) d\lambda}{\int SR_R(\lambda) E_S(\lambda) d\lambda} \frac{\int SR_T(\lambda) E_S(\lambda) d\lambda}{\int SR_T(\lambda) E_{STND}(\lambda) d\lambda} \quad (1)$$

The short circuit current of the test cell, I_{sc}^T , can be corrected for spectral mismatch error to the actual short circuit current using^{12,13}

$$I_{sc} = I_{sc}^T / M \quad (2)$$

This procedure has been used to correct for spectral mismatch in a wide variety of cells, reducing the error in short-circuit current to less than 1% for outdoor measurements and to less than 2% for measurements under a xenon simulator. A summary comparison of measurements on several cells using this technique is presented in Table 1¹⁴. The second procedure omits the two integrals involving $SR_R(\lambda)$ in Eq. 1, and requires absolute $E_S(\lambda)$ measurements. This pro-

GeAs n+pp+

SAMPLE: 8481-2 $V_{oc} = 1.008$ volts

DATE: JUL 23 1984 13:49 $J_{sc} = 23.35$ mA/cm²

TEMP = 28.0 C Fill factor = 85.53 %

AREA = 0.541 cm² Efficiency = 20.1 %

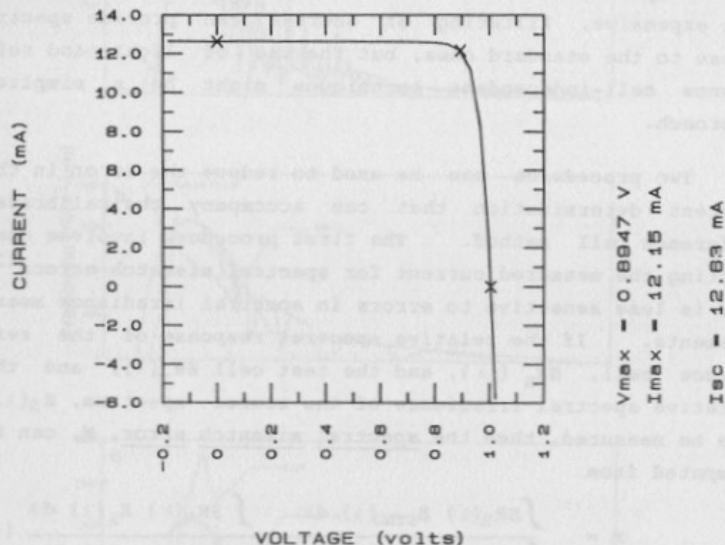


Fig. 4. Current-voltage characteristics under standard test conditions for GaAs solar cell. This high-efficiency cell was fabricated by J.C.C. Fan and Co-workers, MIT-Lincoln Lab.

n+ GaAlAs/GaAs n+pp+
 SAMPLE: 8461-2 Light bias = 12.6 mA
 DATE: NOV 19 1984 5:09p Zero voltage bias
 TEMP = 28.0 C
 AREA = 0.505 cm²

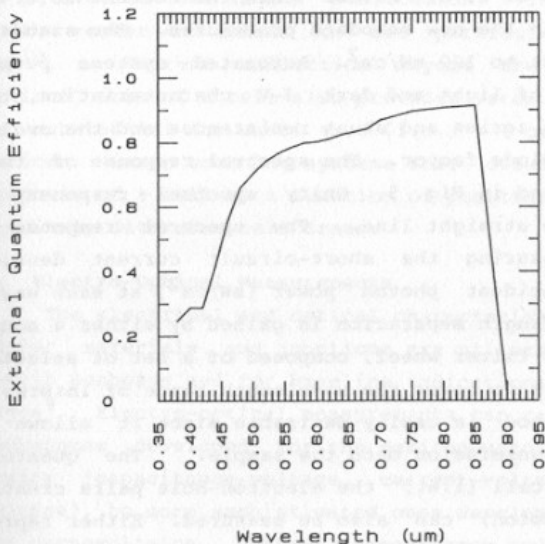


Fig. 5. Spectral response of GaAs solar cell shown in Fig. 4.

cedure does not use a reference cell. Using this revised approach, errors are typically less than 5%.

A typical light current-voltage characteristic is presented in Fig. 4. This cell represents the highest efficiency GaAs cell measured at SERI to date. The test conditions are shown on the figure. It should be noted that a cell temperature of 25 C, rather than the current 28 C, is being proposed in the new standard procedures. The standard irradiance is set to 100 mW/cm². Automated systems permit the measurement of light and dark J-V characteristics, the determination of series and shunt resistances and the evaluation of the diode factor. The spectral response of this cell is presented in Fig. 5. Unity spectral response is indicated by the straight line. The spectral response is derived by measuring the short-circuit current density (mA/cm²) per incident photon power (mW/cm²) at each wavelength⁶. Wavelength separation is gained by either a monochromator or a filter wheel, composed of a set of selected bandpass filters to cover the wavelength range of interest. The latter method is usually desirable since it allows a greater light transmission onto the sample. The quantum-efficiency of a cell (i.e., the electron-hole pairs created per incident photon) can also be measured. Either representation provides diagnostic information on the cell's behavior that is useful for device engineers. Typically, absolute spectral response can be measured with an accuracy of + 5% and repeatability of + 1%.

Of the errors encountered in measuring the efficiencies of research cells, that relating to the determination of cell area is the most severe¹⁵. The conversion efficiency of a solar cell is inversely proportional to the cell area (through the illuminated current density). Thus, in order to measure efficiency accurately, it is necessary to have an accurate measurement of the cell area. If the cell substrate does not define the area (i.e., more than one cell is fabricated on a single substrate), the active cell area and efficiency are open to question. For measuring the performance of cells, the best (undisputed) method is to use the

total cell area, including the area covered by grids or contacts. "Active area" cell efficiencies are sometimes quoted, and seems acceptable only if the researchers are attempting to compare material quality and their own fabrication technologies (e.g., gridding) are not state-of-the-art. However, the problem comes when the researcher "inadvertently" fails to report that his cell efficiency is an active area one in his publication. This is misleading to the reader and unfair to the particular cell technology¹⁰. Current collection beyond the "geometrically-defined" area of a cell also provides error. This error can be substantial for small area (i.e., $< 1 \text{ cm}^2$) research-type devices. Laser scanning systems that determine the photo-response of a cell as a function of position are utilized to precisely determine cell areas.

3. Electro-Optical Measurements

The electrical and optical characterization of semiconductor materials and junctions are utilized both for diagnostic purposes and for baseline indications of cell performance⁹. Electro-optical measurements can range from routine techniques developed for the semiconductor electronics industry (capacitance-voltage, current-voltage, conductance-voltage), to more sophisticated ones developed specifically for photovoltaics. Current, capacitance and conductance vs. voltage characteristics provide important information on carrier concentrations, doping profiles, and electronic junction location. Analogue and digital techniques have been developed to provide information as a function of frequency, with measurements beyond 50 MHz now common. Combining these results with current-voltage characterizations, precise determinations of contact resistance and barrier heights (for junctions and defects) are possible.

Although these measurements are considered "textbook-type", the interpretation of the data requires a great deal of experience. Misinterpretation of C-V results is probably the most common mistake found in the literature, since multiple models can be used to explain a given characteristic. Variations of capacitance measurements, such as

deep-level transient spectroscopy (DLTS) and photocapacitance can be used to provide information of the density-of-states within the bandgap and the diffusion length of minority carriers. These fundamental measurements indicate problems with open-circuit voltage and short-circuit current parameters in cells.

The basic optical properties of materials are very important to the modeling engineer/scientist. Because recent photovoltaic research has been directed toward new materials or semiconductor alloys, little or no information on their exact optical parameters is found in the literature. The basic optical properties of materials are determined through a variety of techniques, including ellipsometry, spectrophotometry and photoluminescence. Ellipsometry is used to measure the optical parameters of materials, and the thicknesses of thin films³. Ellipsometric techniques have been developed to determine these properties individually for multiple layer thin-film structures. Transmission, reflection and adsorption coefficients are determined from both ellipsometric and spectrophotometric techniques. Additionally, the optical bandgaps of semiconductors can be evaluated via these methods.

Photoluminescence, or the emission of light due to electronic transitions from and to specific states resulting from characteristic laser excitation, is used to evaluate the quality of a photovoltaic material. Photoluminescence provides information on electronic transitions, including band-to-band and impurity levels. Thus, the bandgap can be determined. However, photoluminescence provides the most sensitive tool to measure the presence of low-level impurities in a material. Impurities in semiconductors such as GaAs and InP have received much attention in the literature, and levels associated with common impurities are more easy to identify. However, less investigated semiconductors such as new photovoltaic materials have had very little photoluminescence research. The interpretation of such spectra is more difficult--especially in semiconductors controlled by intrinsic defect mechanisms. A series of photolumin-

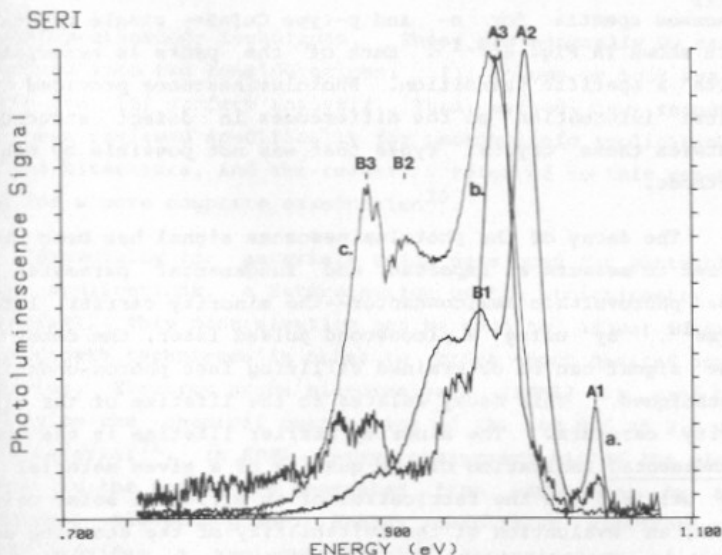


Fig. 6. Photoluminescence spectra of three representative CuInSe_2 crystals, taken at 7 K. (a) $\text{Cu/In} = 1.1$; 1.2% Se deficiency; p-type; (b) $\text{Cu/In} = 0.97$; 0.8% Se deficiency; n-type; (c) $\text{Cu/In} = 0.85$; 2.0% Se deficiency; n-type. (From ref. 17.)

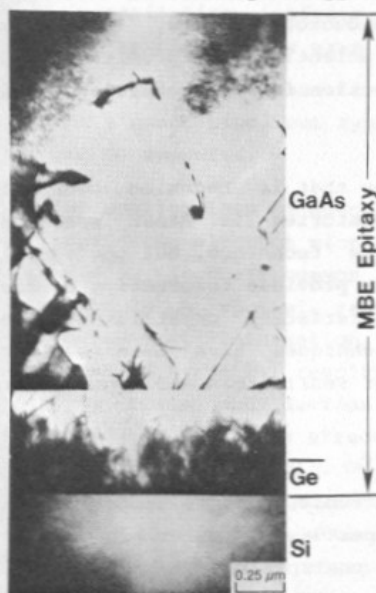


Fig. 7. TEM cross-sectional micrograph of MBE grown Si-Ge-GaAs structure. (From ref. 23.)

escence spectra for n- and p-type CuInSe_2 single crystals are shown in Fig. 6^{16,17}. Each of the peaks is associated with a specific transition. Photoluminescence provided the first information on the differences in defect structure between these crystal types that was not possible by other methods.

The decay of the photoluminescence signal has been utilized to measure an important and fundamental parameter of the photovoltaic semiconductor--the minority carrier lifetime¹⁸. By using a picosecond pulsed laser, the decay in the signal can be determined utilizing fast photon-counting techniques. This decay relates to the lifetime of the minority carriers. The minority carrier lifetime is the most fundamental indication of the quality of a given material to be utilized in the fabrication of an efficient solar cell. Thus, an evaluation of the suitability of the starting material can be made before subjecting it to the time-consuming and costly ensemble of cell fabrication processes. Lifetimes as low as 10 ps can be determined by this method in direct bandgap semiconductors. Information of this type, especially on the III-V semiconductory alloys, is very important to device modeling scientists for predicting cell efficiency and providing direction for high-efficiency cell improvements.

Another laser spectroscopy that is becoming common in semiconductor diagnostic laboratories is Raman spectroscopy¹⁹. This is not a new technique, but one that is finding new applications. It provides information on composition, interactions at interfaces, crystallinity and impurities. Micro-Raman techniques have been developed which permit the examination of small areas and regions near the surface of a device.

4. Materials Characterization

The crystallographic, electronic, defect, topographical, chemical and compositional properties of materials and interfaces, all of which can be controlling entities for cell operation, can be determined using advanced microscopy and

micro-spectroscopy techniques. These can generally be categorized into two considerations: (1) Volume or bulk analysis; and, (2) Surface analysis. These methods have recently been reviewed specifically for photovoltaic applications in the literature, and the reader is referred to this material for a more complete examination²⁰.

Especially for materials being developed for photovoltaic applications, a determination of the stoichiometry is important. This determination can be used to adjust materials growth techniques in order to bring about desired composition. Electron probe microanalysis (EPMA) is used to determine the chemical composition of the top 0.5 to 2.0 μm of a material²¹. In EPMA, X-rays characteristic of the elements in the sample are generated from excitation by an energetic electron probe. Energy dispersive spectroscopy (EDS) provides a semi-quantitative determination of elemental composition. Wavelength dispersive spectroscopy (WDS) has superior sensitivity, better peak resolution and is less disturbed by background noise. Thus, WDS provides better quantitative analysis. With computer control, as many as 50 samples can be examined per day--providing rapid analysis. Elemental sensitivity varies due to matrix effects and element type, but typically concentrations to 0.1 at.-% can be measured.

The applications of scanning electron microscopy (SEM) and transmission electron microscopy (TEM) have been widely publicized²². In their common applications, SEM (with approximately 30 \AA spatial resolution) is used to provide three-dimensional information on topography, and TEM (with better than 3 \AA spatial resolution), information on defects within materials and devices. A cross-sectional TEM micrograph of a Si/Ge/GaAs structure grown by molecular beam epitaxy is presented in Fig. 7²³. This structure is used in the fabrication of multiple-junction solar cells, with the Ge layer providing a lattice match for the growth of the GaAs, and inhibiting the propagation of dislocations into the III-V layer.

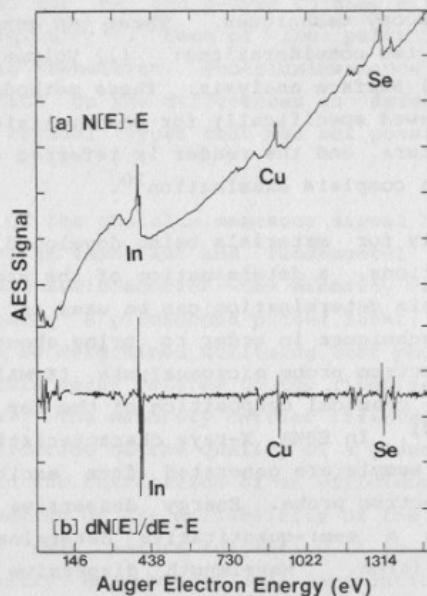


Fig. 8. AES survey scans of CuInSe_2 thin film; (a) direct $(N(E)-E)$ Auger electron spectrum; (b) differentiated spectrum.

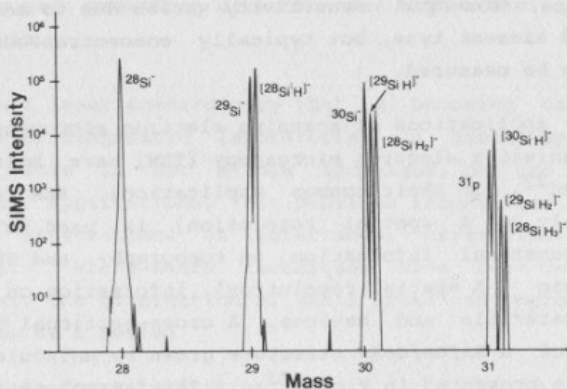


Fig. 9. SIMS spectra of amorphous Si:H cell layer doped with P. High mass resolution enables separation and identification of the iso-mass peaks.

Electron-probe instruments, such as the EMPA and SEM, can be used for complementary microelectrical characterization techniques. Electron-beam induced current (EBIC) utilizes the scanning of the focussed electron beam across a sample, while monitoring the induced electronic current. Changes in current collection can be spatially-resolved²⁴. These changes in current collection locate the position of depletion regions, such as junctions and grain boundaries. References to EBIC data applied to photovoltaics are common in the literature^{20,25}. However, the researcher should be careful since (as with many techniques employing energetic electron probes) it is possible to create artifacts that are not device inherent.

An expanding area of materials and device characterization is that of surface analysis²⁰. These techniques examine the topmost 3-50 Å of a material for elemental composition. They utilize a variety of input probes (electrons, ions, X-rays, and photons) and detect several output particles (electrons, ions)²⁰. The common techniques are Auger electron spectroscopy (AES) (electrons in - electrons out), X-ray photoelectron spectroscopy (XPS or ESCA) (X-rays in - electrons out), secondary ion mass spectrometry (SIMS) (ions in - ions out) and ultraviolet photoelectron spectroscopy (UPS) (ultraviolet radiation in - electrons out). The output of these techniques provide fingerprints that are indicative of the elemental species being examined. A representative AES spectrum for CuInSe_2 is presented in Fig. 8. The energy location of each peak represents an energy transition for a given atom. Handbooks are available to help interpret such data. Each surface analysis technique has its own particular strength²⁰. AES uses an incident electron probe, and thus can provide high spatial resolution and mapping of impurities on surfaces. XPS is the least damaging, since it employs X-rays as the input probe. Additionally, chemical bonding information is gained since core electrons are analyzed. SIMS provides the most sensitivity to trace elements. For example, B in Si can be detected to about $10^{14}/\text{cm}^3$. (This compares to about 0.1 at.-% using

either AES or XPS.) SIMS can also provide high mass resolution. Fig. 9 shows the mass 31 peak for an amorphous hydrogenated Si cell. The P dopant and the various Si-H peaks can be resolved. This allows for the quantification of H in amorphous Si, an important determination for that solar cell technology. Depth-profile information can be gained with these techniques. For AES and XPS, sputter etching can be combined with the relevant spectroscopy to determine the depth profile of the elemental species. In SIMS, the sputtering is inherent to the process. Recently, volume-indexing of the SIMS data has been accomplished, and provides for the first time the ability to view maps of elemental impurities and molecular species on internal interfaces using a single dynamic SIMS analysis²⁶.

5. Summary

The purpose of this paper has been to provide a survey of characterization techniques used in photovoltaic research and development. This survey is not exhaustive, but representative of common methods in each of the defined measurement areas. Two observations should be emphasized. First, the techniques themselves are not sufficient to the solution of a problem. Expertise is required for the proper application of the method and the interpretation of results. Second, the complementary application of two or more diagnostic techniques is usually required for the unambiguous solution of a materials/device problem.

Acknowledgements

The author would sincerely like to thank the members of the SERI Photovoltaic Devices and Measurements Branch who contributed their work, expertise and patience to this publication. Special acknowledgement is given to Keith Emery and Carl Osterwald who are responsible for the development of the advanced cell efficiency measurement techniques and serve as guardians for accurate efficiency reports for SERI and the U.S. DOE Program. This work was supported by the U.S. Department of Energy, through a subcontract to the Solar Energy Research Institute (DE-AC02-83CH10093).

References

1. L.L. Kazmerski, Rev. Brasil. Apl. Vac. 3 (1983) 171.
2. SERI Photovoltaic Advanced Research and Development, SERI/SP 281-2235, SERI, Golden, Colo., 1984.
3. See, for example, Solar Cells 1 (Part I and II) (1980) 113-346.
4. The SERI Photovoltaic Devices and Measurements Laboratories, SERI/SP 281-1940, SERI, Golden, Colo., 1983.
5. L.L. Kazmerski, Appl. Surf. Sci. 7 (1981) 55.
6. See, for example, A.L. Fahrenbruch and R.H. Bube, Fundamentals of Solar Cells, Academic Press, New York, 1983.
7. R.J. Matson, K.A. Emery and R.E. Bird, Solar Cells 11 (1984) 105.
8. C.R. Osterwald, Proc. 18th IEEE Photovoltaic Spec. Conf., Las Vegas, October, 1985, IEEE, New York (in-press).
9. H. Curtis, Terrestrial Photovoltaics Measurement Procedures, NASA Techn. Memo. TM 73702, NASA, Cleveland, Ohio, 1977. Also, Proc. 14th IEEE Photovoltaic Spec. Conf., IEEE, New York, 1980, pp. 500-505.
10. C.J. Riordan, "Spectral Solar Irradiance Models and Data Sets", Photovoltaics and Insolation Measurements Workshop, June 30 - July 3, 1985, SERI/CP 215-2740, pp. 11-14.
11. Standard Method for the Calibration and Characterization of Nonconcentrator Terrestrial Photovoltaic Reference Cells Under Direct Normal Irradiance, ASTM Draft Doc. 130 R10 E-44.09.03, 1983.
12. C.R. Osterwald, "Translation of Device Performance Measurements", Photovoltaics and Insolation Measurements Workshop, June 30 - July 3, 1985, SERI/CP 215-2740, pp. 27-28.
13. K.A. Emery, "Solar Simulators and I-V Measurement Methods", Photovoltaics and Insolation Measurements Workshop, June 30 - July 3, 1985, SERI/CP 215-2740, pp. 23-24.
14. K.A. Emery, C.R. Osterwald, Proc. 18th IEEE Photovoltaic Spec. Conf., Las Vegas, October 1985, IEEE, New York (in-press).
15. C.R. Osterwald and K.A. Emery, Solar Cells 10 (1983) 1.
16. F. Abou-Elfotouh, D.L. Dunlavy and L.L. Kazmerski, Proc. 17th IEEE Photovoltaic Spec. Conf., IEEE, New York, 1984, pp. 1410-1411.
17. F. Abou-Elfotouh, D.J. Dunlavy, D. Cahen, R. Noufi, L.L. Kazmerski and K.J. Bachmann, Prog. Cryst. Growth, 10 (1985) 365.
18. M.A. Green, Solar Cells 11 (1984) 147.
19. F.H. Pollak and R. Tsu, Proc. of SPIE, Vol. 452, SPIE, Bellingham, Wash., 1984, pp. 26-43.
20. L.L. Kazmerski, "Advanced Materials and Device Analytical Techniques", in Advances in Solar Energy, Vol. III, K. Boer, Ed., Plenum Press, New York, 1985 (in-press).

21. J.I. Goldstein, Scanning Electron Microscopy and X-Ray Analysis, Plenum Press, New York, 1981.
22. See, for example, Scanning Electron Microscopy/1983/ I-IV, SEM, Inc., O'Hare, Ill., 1983.
23. P. Sheldon, K.M. Jones and R.E. Hayes, Appl. Phys. Lett. 1984.
24. H.J. Leamy, J. Appl. Phys. 53 (1982) R51.
25. P.E. Russell, O. Jamjoum, R.K. Ahrenkiel, L.L. Kazmerski, R.A. Mickelsen and W.S. Chen, Appl. Phys. Lett. 40 (1982) 995.
26. L.L. Kazmerski, Rev. Brasil. Apl. Vac. (This Issue).